TOXICOLOGICAL SCIENCES **105(1)**, 97–105 (2008)
doi:10.1093/toxsci/kfn109
Advance Access publication June 3, 2008

Cellular Imaging Predictions of Clinical Drug-Induced Liver Injury

Jinghai J. Xu,*,†,[1] Peter V. Henstock,‡ Margaret C. Dunn,*,† Arthur R. Smith,*,† Jeffrey R. Chabot,† and David de Graaf†,[2]

Predictive Toxicology; †Systems Biology; and ‡Target & Mechanism Informatics, Pfizer Research Technology Center, Pfizer Global Research and Development, Cambridge, Massachussetts 01239

Received April 2, 2008; accepted May 22, 2008

Drug-induced liver injury (DILI) is the most common adverse event causing drug nonapprovals and drug withdrawals. Using drugs as test agents and measuring a panel of cellular phenotypes that are directly linked to key mechanisms of hepatotoxicity, we have developed an *in vitro* testing strategy that is predictive of many clinical outcomes of DILI. Mitochondrial damage, oxidative stress, and intracellular glutathione, all measured by high content cellular imaging in primary human hepatocyte cultures, are the three most important features contributing to the hepatotoxicity prediction. When applied to over 300 drugs and chemicals including many that caused rare and idiosyncratic liver toxicity in humans, our testing strategy has a true-positive rate of 50–60% and an exceptionally low false-positive rate of 0–5%. These *in vitro* predictions can augment the performance of the combined traditional preclinical animal tests by identifying idiosyncratic human hepatotoxicants such as nimesulide, telithromycin, nefazodone, troglitazone, tetracycline, sulindac, zileuton, labetalol, diclofenac, chlorzoxazone, dantrolene, and many others. Our findings provide insight to key DILI mechanisms, and suggest a new approach in hepatotoxicity testing of pharmaceuticals.

Key Words: **liver injury; idiosyncratic hepatotoxicity; hepatitis; mechanism of organ toxicity; *in vitro in vivo* correlations; pharmacokinetic scaling; hepatotoxicity testing.**

Advances in modern drug therapy have saved and improved many human lives. However, adverse drug reactions represent a major challenge for healthcare professionals, drug regulators, and pharmaceutical companies. Drug-induced liver injury (DILI), in particular, is an alarming public health problem. It is the leading cause in acute liver failures that necessitate organ transplants, safety recalls from the world-wide pharmaceutical market, nonapprovable decisions regarding new drug applications (NDAs), and internal drug development failures among all major pharmaceutical companies (Giacomini *et al*., 2007; Holt and Ju, 2006; Kaplowitz, 2005; Lee, 2003; Navarro and Senior, 2006; Schuster *et al*., 2005; Senior, 2007; Zimmerman, 2000). If predictive cellular systems can be developed and applied to identify a significant number of hepatotoxic drugs with a high degree of specificity, it would undoubtedly improve the safety profile of new therapies and impact the well being of both humans (minimize unsafe drug exposure to patients) and animals (support the replacement, refinement and reduction of animal usage). Recently, well-defined and characterized primary cultures of human hepatocytes were developed and demonstrated to maintain the differentiated functions of liver metabolism and transport (Bi *et al*., 2006; Davila *et al*., 2007; Gross-Steinmeyer *et al*., 2005; Hewitt *et al*., 2007; Hoffmaster *et al*., 2004; LeCluyse *et al*., 2005; Page *et al*., 2007). We report here that by applying this primary cell culture system and measuring a panel of signals directly linked to key mechanisms of liver injury (Holt and Ju, 2006; Lee, 2003; Xu *et al*., 2004) using high content imaging approaches, we can make significant improvements over existing capabilities for predicting drugs that can cause liver injury including idiosyncratic hepatotoxicity.

MATERIALS AND METHODS

Materials. Most of the drugs and chemicals were purchased from Sigma Chemicals (St Louis, MO) or Sequoia Research Products (Pangbourne, UK). In a small number of cases where such chemicals were not commercially available, they were obtained from the Pfizer chemical sample bank (Groton, CT). Human hepatocytes were obtained from CellzDirect (Durham, NC), as well as human hepatocyte media and media supplements. BD BioCoat plates and Matrigel were purchased from BD BioSciences (Billerica, MA). All fluorescent probes were purchased from Molecular Probes (Eugene, OR), except for 1,5-bis{[2-(di-methylamino) ethyl]amino}-4,8-dihydroxyanthracene-9,10-dione (DRAQ5), which was from Biostatus (Shapshed, UK).

Drug classifications and pharmacokinetic database. Drug classification based on clinical data of hepatotoxicity (Kaplowitz, 2005; Lee, 2003; Stricker, 1992; Zimmerman, 1999) was verified by an automated PubMed search tool commercially available from QUOSA (Brighton, MA). QUOSA enables automated full-text searches of any number of drugs AND any number of classical terminologies for liver injury (i.e., liver injury, hepatotoxicity, hepatitis, hepatic damage, and variations thereof), within PubMed. The search was conducted in November, 2005. Therapeutic exposure levels were obtained from a combination of literature search and commercially available databases (PubMed, Physicians' Desk Reference, Prous, and Pharmapendium). The therapeutically active average plasma maximum concentration (Cmax) values upon single-dose administration at commonly recommended therapeutic doses

[1] Current address: Department of Automated Biotechnology, Merck & Co., 140 Wissahickon Ave., North Wales, PA 19454.

[2] To whom correspondence should be addressed at Systems Biology, Pfizer Research Technology Center, Pfizer Global Research and Development, 620 Memorial Drive, Cambridge, MA 01239. E-mail: david.degraaf@pfizer.com.

were collated. In cases where multiple recommended doses are available, the average total Cmax corresponding to a single administration at the median dose was used. In a small fraction of cases where human therapeutic Cmax values were not available (e.g., the development of a drug candidate was stopped before any human Cmax value could be obtained), the human total Cmax was assumed to be 1μM.

Human hepatocyte imaging assay technology. Freshly isolated or cryopreserved (but long-term culturable) human hepatocytes were obtained commercially from CellzDirect (Durham, NC). For image assays, the hepatocytes used need to be "imaging-quality"—that is, confluent monolayer cultures without excessive intracellular lipid vacuoles. About 60,000 viable hepatocytes were plated on collagen I-coated BD BioCoat 96-well plates in hepatocyte plating medium (Dulbecco's Minimal Essential Medium, 5% fetal bovine serum, 50 unit/ml penicillin, 50 μg/ml streptomycin, 4 μg/ml bovine insulin, 4mM L-glutamine, 1μM trichostatin A, and 1μM dexamethasone). After 3 h, the nonattached cells were shaken and aspirated off the plate, and the medium was changed to hepatocyte culturing medium without phenol red (Williams E medium supplemented with 6.25 μg/ml insulin, 6.25 μg/ml transferrin, 6.25 ng/ml selenious acid, 1.25 mg/ml bovine serum albumin, 5.35 μg/ml linoleic acid, 15mM of 4-(2-hydroxyethyl)-1-piperazineethanesulfonic acid, 50 unit/ml penicillin, 50 μg/ml streptomycin, 4mM L-glutamine, 1μM trichostatin A, and 0.1μM dexamethasone). On the second day, the Matrigel overlay was applied by changing the medium to ice-chilled hepatocyte culturing medium containing ice-cold Matrigel at a final concentration of 0.25 mg/ml. On the third day, the cells were treated by a compound of interest or vehicle (0.1% dimethyl sulfoxide [DMSO]). All compounds were initially solubilized in 100% DMSO. They were diluted in the same hepatocyte culturing medium as above, but with phenol red and 5% fetal bovine serum, to a final DMSO concentration of 0.l%. The inclusion of phenol red in this step was to allow a facile way to identify and exclude a small number of compounds that might alter the pH of the buffered medium. The inclusion of 5% serum was to facilitate both drug solubility and correlation with total therapeutic Cmax *in vivo* (*vide infra*). After 24 h of incubation (37°C, 5% CO_2, 100% humidity), the medium was removed and the cells were stained by fluorescent probes in the same hepatocyte culturing medium without serum or phenol red. The fluorescent probes used were tetramethyl rhodamine methyl ester (TMRM) (0.02μM, 1 h), DRAQ5 (45μM, 30 min), 5-(and-6)-chloromethyl-2′7′-dichlorodihydrofluorescein diacetate acetyl ester (CM-H_2DCFDA) (10μM, 30 min), and finally monochlorobimane (mBCl) (80μM, 5 min). The TMRM, DRAQ5, and CM-H_2DCFDA were incubated together with the cells for the first 30 min, followed by TMRM alone for 25 min in the cell culture incubator, then finally TMRM with mBCl for 5 min in the environmental chamber of the Kinetic Scan Reader. Automated live-cell multispectral image acquisition was performed on the same Kinetic Scan Reader using a ×20 objective (Cellomics, Pittsburgh, PA). The mBCl probe was prewarmed to 37°C and added live on the deck of the instrument. The fluorescence images were captured according to the optimal excitation and emission wavelengths of each probe using an XF93 filter (Omega Optical, Brattleboro, VT):

- 655 ± 15 and 730 ± 25 nm for DRAQ5 (channel 1—nuclei/lipids), exposure time 0.7 s.
- 475 ± 20 and 515 ± 10 nm for CM-H2DCFDA (channel 2—reactive oxygen species [ROS]), exposure time 0.3 s.
- 549 ± 4 and 600 ± 12.5 nm for TMRM (channel 3—mitochondrial membrane potential [MMP]), exposure time 0.05 s.
- 365 ± 25 and 515 ± 10 nm for mBCl (channel 4—glutathione [GSH]), exposure time 0.4 s.

To capture enough cells (> 500) for analysis, six image fields starting at the center of a well were collected from each well. Image analysis was performed using the ImagePro Plus software (Media Cybernetics, Bethesda, MD). A series of measurements from the nuclei and lipids, ROS, TMRM, and GSH channel images were obtained for each drug. They were: nuclei count, nuclei area, lipid intensity, ROS intensity, TMRM intensity, GSH content, GSH area, and GSH average pixel intensity. The sum of these numerical measurements from the six image fields within the same well were divided by the sum of nuclei count from the same six image fields to obtain values that were standardized by cell number. The values from the same treatment (e.g., duplicate wells) were averaged and then normalized by the average values from 16 vehicle-treated wells. Hence, all the vehicle-treated wells in a 96-well plate will have an average value of 1 in all imaging outputs and each drug-treated response in values relative to 1.

Statistical analysis. Statistical analysis of the predictivity of the human hepatocyte imaging assay technology (HIAT) was conducted using receiver-operating characteristic (ROC) curves, Boolean logic, and random forest analysis.

The ROC curve was generated by computing the paired true- and false-positive rates for all possible thresholds for each imaging profile value (Lasko *et al*., 2005). The best predictions occur toward the top-left corner indicative of high true-positive and low false-positive rates. This approach generated a threshold where the false-positive rate is zero and the true-positive rate is a fraction between 0 and 1 for each imaging measurement. This threshold was then applied to each imaging measurement to score that measurement either as positive or negative. To increase the overall assay sensitivity, these binary scores were combined using Boolean logic OR (Duda *et al*., 2000), to obtain "Human Hepatocyte (HH) Imaging Final Score." This procedure assigned a DILI positive label to a compound if any single imaging measurement produced a positive score by the single assay threshold mentioned above.

Standard random forest machine learning algorithm was applied as described (Breiman, 2001). A total of 2500 decision trees were trained based on the imaging profile data. The trees were each trained on 63.2% of the data with the remainder used for testing (Breiman, 2001). Each compound was then scored by fraction of positive predictions it received from the trees on which it had not been trained to form an out-of-bag prediction score. The score obtained for each compound was then used to produce an ROC curve using all possible thresholds as described above.

RESULTS

Drug Classifications and Pharmacokinetic Database

We first developed a database of more than 300 drugs and chemicals with a classification scheme based on clinical data of hepatotoxicity. Our DILI positive drugs include those (1) withdrawn from the market mainly due to hepatotoxicity (e.g., troglitazone), (2) not marketed in the United States due to hepatotoxicity (e.g., nimesulide), (3) received black box warnings from the Food and Drug Administration (FDA) due to hepatotoxicity (e.g., dantrolene), (4) marketed with hepatotoxicity warnings in their labels (e.g., telithromycin), (5) others that had well-known associations to liver injury and had a significant number (> 10) of independent clinical reports of serious hepatotoxicity that meet the criteria of Hy's Law (Temple, 2006) (e.g., sulindac, diclofenac), and (6) a small number of Pfizer internal drug candidates whose development were ceased mainly due to hepatotoxicity concerns (largely as the result of preclinical animal toxicology data). This small number of internal drug candidates did not reach the NDA stage; hence, their identities were codified by compound numbers. Drugs that do not meet any of the above positive criteria are classified as DILI negatives. Since every drug can exhibit some toxicity at high enough exposure (i.e., the notion of "dose makes a poison" by Paracelsus; Guggenheim, 1993),

we searched therapeutic exposure levels in the literature and collated the therapeutically active average plasma maximum concentration (Cmax) values upon single-dose administration at commonly recommended therapeutic doses. Our entire DILI drug database, including DILI classifications, Cmax values, and Cmax references, can be found in Supplementary Table 1 on line.

Human Hepatocyte Imaging Assay Technology

To measure a panel of signals that are directly linked to key mechanisms of liver injury simultaneously, we applied multispectral live-cell imaging of human hepatocytes upon drug treatment by costaining with multiple fluorescent probes. By examining these high content imaging outputs, useful mechanistic information can be extracted (Fig. 1). Our findings are in accordance with the known mechanisms of DILI by these drugs: perhexiline can cause nonalcoholic steatohepatitis by a combination of mitochondrial dysfunction and lipid accumulation (Fig. 1e) (Berson *et al*., 1998); and oxidative stress has been implicated in nimesulide-induced liver injury (Fig. 1b) (Boelsterli, 2002). Our findings also suggest novel mechanisms previously undocumented in the literature. For example, the precise mechanism of nefazodone-induced toxicity is still unclear, with both reactive metabolite formation (Kalgutkar *et al*., 2005) and transporter inhibition (Kostrubsky *et al*., 2006) reported. Our imaging results suggest that nefazodone induces cytoplasmic lipid accumulation, oxidative stress, mitochondrial abnormality, and intracellular GSH depletion (Fig. 1d). Recently, the role of mitochondria in nefazodone-induced liver injury was substantiated by detailed *in vitro* mechanistic studies (Dykens *et al*., 2008). Likewise, our results highlight the importance of mitochondria, GSH, and lipidosis in telithromycin-induced hepatotoxicity (Fig. 1c) (Ross, 2007).

These multichannel image outputs can be further quantified by automated image analysis algorithms using standardized

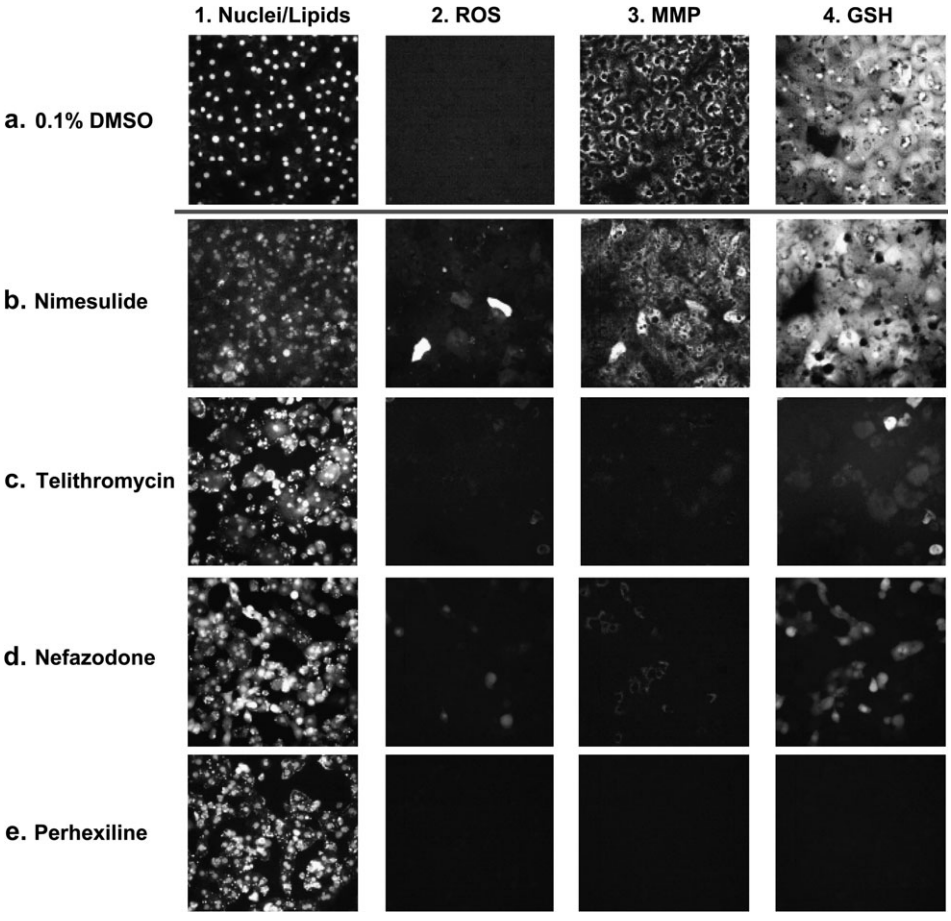

FIG. 1. Representative images from the human HIAT, in which human hepatocytes were treated with: (a) vehicle (0.1% dimethyl sulfoxide or 0.1% DMSO in hepatocyte culture medium), (b) nimesulide, (c) telithromycin, (d) nefazodone, (e) perhexiline. Each set of images were obtained from the same image field, with column 1, 2, 3, 4 being images of nuclei/lipids, ROS, MMP, and GSH, respectively. Each drug was treated for 24 h at 100-fold therapeutic Cmax (as listed in Supplementary Table 1). Nimesulide caused a significant increase in ROS. Telithromycin, nefazodone and perhexiline caused significant decrease in MMP and GSH. Some lipid droplets were also visible in nefazodone and perhexiline treated hepatocytes, as indicated by the lipophilic probe DRAQ5 that normally only stains the nuclear DNA.

image analysis procedures measuring the intensity and area or size of any object of interest. A series of measurements from these multispectral images was hence made for each drug, resulting in a series of imaging outputs representing an ''imaging profile'' for a particular drug. In Table 1, vehicle-treated control samples have an average value of 1 in all imaging outputs and each drug-treated response in values relative to 1. Using binary heat maps, researchers can rapidly decipher the types of hepatocyte injury posed by the drug of interest. Of the 30 drugs listed here, the first 11 drugs were known to cause serious DILI in humans. Perhexiline (Shah, 2006), troglitazone (Scheen, 2001), nefazodone (Choi, 2003) were withdrawn from the market due to hepatotoxicity or DILI concerns. Tetracycline was known to be more hepatotoxic than other antibiotics such as penicillin, which had a well-defined record of low hepatotoxicity (Thiim and Friedman, 2003). Nimesulide and sulindac (Aithal and Day, 2007) were well-known drugs that caused higher incidences of liver injuries than other nonsteroidal anti-inflammatory drugs such as aspirin or ketotifen. Zileuton, labetalol, diclofenac, chlorzoxazone, and dantrolene were explicitly second-line therapies or bear serious warnings because of liver toxicity (Temple, 2001). These drugs were identified as positive in the hepatocyte imaging assay. On the other hand, drugs that are considerably safer to human livers in clinical usage (i.e., those with a DILI label of N, for Negative) were consistently identified as negative in the assay (Table 1). The entire imaging profile data for the 344 drugs and chemicals in our DILI drug database, can be found in Table 2 of the Supplementary Data online.

Statistical Analysis

We next examined the sensitivity (defined as the fraction of correctly predicted positives to all true positives in the clinic) and specificity (defined as the fraction of correctly predicted negatives to all true negatives in the clinic) of this imaging-based assay. Such an approach utilizes biological knowledge of the assay to set thresholds from which predictive toxicity is assigned (e.g., an increase in lipid and ROS corresponds to toxicity, as well as a decrease in nuclei count, mitochondria potential, and GSH). Figure 2 shows an exhaustive approach using the ROC curve containing the paired true- and false-positive rates for all possible thresholds for each imaging measurement (Lasko *et al*., 2005). The best predictions occur toward the top-left corner indicative of high true-positive and low false-positive rates. Notice in Figure 2 that each individual assay has a threshold where the false-positive rate is zero and the true-positive rates are still between 0.1 and 0.3. In one approach, we utilized these ''zero-false-positive thresholds'' to convert the assay measurements into binary toxicity scores. These binary scores can then be combined using Boolean logic (Duda *et al*., 2000). A simple but intriguing result was obtained using a logical OR of eight assays shown as the ''HH Imaging Final Score'' (top black dashed line) in Figure 2, and in the second rightmost column of Table 1.

While the logical OR method combining all the imaging profile results provides insight on potential mechanisms of drug toxicity retrospectively, it does not have the rigor of a testing and training paradigm that suggests the future performance by ''predicting'' compounds not used to formulate the prediction. We next used a random forest machine learning algorithm (Breiman, 2001) to assess the predictive performance. Each compound was scored by fraction of positive predictions it received from the trees which had not been trained using it to form an out-of-bag prediction score. The scores can then be used for predictions and produce ROC assessments as shown in the top red dashed line in Figure 2. Between the two top-left corners of black and red dashed lines, the HIAT produced a combined true-positive rate of 50–60% and a remarkably low false-positive rate of 0–5% (Fig. 2). Three features contributed most to the overall random forest model. They are, in decreasing order of importance: MMP, ROS, and reduced intracellular GSH level. Cell number, or nuclei count, is among the least discriminative feature, indicating the assay is not measuring cell loss (a simple measure of cytotoxicity).

DISCUSSIONS

The goal of our study is to apply simultaneous multispectral live-cell imaging investigation on primary cultures of human hepatocytes to derive a set of imaging measurements that is predictive of drugs' ultimate outcome of DILI in the clinical setting. Even though we have not exhaustively examined all drugs that have ever been marketed to date, nor have we measured all cellular imaging parameters as deemed possible by a combination of cellular stains and microscopic optics, several insights were already gained by our investigation. These insights have important implications for *in vivo* correlations of DILI from the perspectives of concentration-effect and mechanisms of liver toxicity.

Pharmacokinetic Considerations: What is Clinically Relevant Concentration to Test In Vitro?

From the outset, to identify an idiosyncratic hepatotoxic drug with a serious hepatotoxic event happening in less than 1 in 1000 patients is an Achilles' task. In essence we need to predict a population's outlier response rather than its mean response, using a single *in vitro* cell type obtained from a limited pool of donors. The only way possible, without testing more than 3000 different patients (FDA's ''rule of 3''; Powers, 2007), is to use reasonably well-accepted uncertainty scaling factors. We used a scaling factor of sixfold to account for population Cmax variability from the average therapeutic Cmax that we collated from the literature, to account for patient genetic (such as metabolic enzymes and transporters) and epigenetic factors (such as age and pre-existing disease) which affect drug clearances (Dorne *et al*., 2005). Another sixfold

TABLE 1
The "Imaging Profile" Data from the HIAT, for a Selective List of 30 Drugs

Drug	DILI label	Nuclei count (< 0.4 = positive)	Nuclei area (< 0.4 = positive)	ROS intensity (> 2.5 = positive)	TMRM intensity (< 0.4 = positive)	Lipid intensity (> 2.5 = positive)	GSH content (< 0.4 = positive)	GSH area (< 0.65 = positive)	GSH average pixel intensity (< 0.4 = positive)	HH imaging final score (logical OR of eight measures)	Human_ Cmax (μg/ml)
0.1% DMSO	N	**1.00**	**1.00**	**1.00**	**1.00**	**1.00**	**1.00**	**1.00**	**1.00**	N	
Perhexiline	P	**0.82**	**0.91**	**0.00**	*0.00*	**1.48**	*0.01*	*0.02*	**1.08**	P	**0.6**
Troglitazone	P	**0.71**	**0.85**	**0.00**	*0.01*	*2.90*	*0.01*	*0.02*	**1.08**	P	**2.82**
Nefazodone	P	**0.45**	**0.52**	**0.00**	*0.04*	**1.81**	*0.01*	*0.03*	**2.10**	P	**0.4**
Tetracycline	P	**1.04**	**1.06**	*430*	*0.10*	*2.90*	**1.13**	**0.82**	**1.97**	P	**9.3**
Nimesulide	P	**0.96**	**0.92**	*27.3*	**1.43**	*2.86*	**0.88**	**0.98**	**0.87**	P	**6.5**
Sulindac	P	**1.14**	**1.08**	*14.2*	**0.69**	**0.79**	**0.63**	**0.81**	**0.66**	P	**11.4**
Zileuton	P	**1.08**	**1.01**	*4.83*	**1.32**	*3.46*	**0.92**	**0.67**	**2.16**	P	**3.1**
Labetalol	P	**0.89**	**0.81**	*4.88*	**0.70**	*5.10*	**1.41**	**0.97**	**1.89**	P	**0.88**
Diclofenac	P	**0.61**	**0.70**	*35.3*	**0.98**	**1.86**	**1.91**	**1.22**	**1.00**	P	**2.4**
Chlorzoxazone	P	**0.48**	**0.74**	*8.39*	**0.78**	**1.70**	**1.01**	**1.65**	**1.31**	P	**0.5**
Dantrolene	P	**0.72**	**0.78**	*8.54*	**1.23**	**1.58**	**1.57**	**1.17**	**0.98**	P	**1.24**
Amitriptyline	N	**0.96**	**1.00**	**0.30**	**1.26**	**1.36**	**1.06**	**0.97**	**0.96**	N	**0.03**
Pioglitazone	N	**1.13**	**1.11**	**0.88**	**1.69**	**1.38**	**0.57**	**0.87**	**0.87**	N	**1.1**
Rosiglitazone	N	**0.66**	**0.79**	**0.44**	**1.04**	**1.66**	**1.52**	**1.38**	**1.13**	N	**0.4**
Primidone	N	**0.96**	**0.91**	**0.62**	**0.90**	**1.19**	**0.75**	**0.95**	**0.91**	N	**1**
Penicillin	N	**0.91**	**0.98**	**0.29**	**1.31**	**1.32**	**0.67**	**1.07**	**0.61**	N	**2.7**
Melatonin	N	**0.97**	**0.96**	**0.68**	**0.95**	**0.93**	**0.91**	**1.00**	**1.00**	N	**0.006**
Nadolol	N	**0.95**	**0.99**	**0.44**	**2.07**	**0.92**	**0.91**	**1.04**	**0.89**	N	**0.1**
Ketotifen	N	**1.02**	**1.01**	**0.60**	**1.00**	**0.88**	**0.90**	**0.94**	**1.00**	N	**0.0004**
Paromomycin	N	**1.00**	**1.02**	**1.02**	**1.66**	**0.93**	**1.23**	**0.99**	**0.99**	N	**23**
Sumatriptan	N	**1.13**	**1.10**	**0.26**	**1.18**	**0.86**	**0.76**	**0.87**	**0.85**	N	**0.08**
Famotidine	N	**1.20**	**1.15**	**0.47**	**1.15**	**0.89**	**0.96**	**0.84**	**0.91**	N	**0.1**
Tacrine	N	**0.86**	**0.91**	**0.48**	**1.14**	**1.30**	**1.14**	**1.08**	**0.84**	N	**0.02**
Simvastatin	N	**0.72**	**0.84**	**0.02**	**0.81**	**1.46**	**1.35**	**1.32**	**0.96**	N	**0.01**
Aspirin	N	**1.04**	**1.00**	**0.58**	**1.25**	**0.87**	**0.62**	**0.94**	**0.50**	N	**1**
Fluoxetine	N	**1.05**	**1.07**	**1.46**	**0.79**	**0.84**	**0.59**	**0.91**	**0.83**	N	**0.015**
Propranolol	N	**1.12**	**1.05**	**0.50**	**1.08**	**0.89**	**0.76**	**0.87**	**0.70**	N	**0.05**
Raloxifene	N	**1.15**	**1.04**	**0.17**	**0.76**	**0.89**	**1.10**	**0.83**	**1.06**	N	**0.0005**
Paroxetine	N	**1.12**	**1.04**	**0.38**	**0.83**	**0.85**	**0.72**	**0.90**	**0.77**	N	**0.02**
Buspirone	N	**0.99**	**1.00**	**1.02**	**1.13**	**0.98**	**0.68**	**0.98**	**1.14**	N	**0.002**

Note. The binary heat map was produced by thresholds that best differentiated the DILI negative from positive drugs (the threshold used was listed under the heading for each measurement). Bold-faced values indicate that the imaging measurement is within the DILI negative threshold, italic values indicate that the measurement falls outside of the DILI negative threshold (i.e., becomes positive). The second rightmost column indicates the combined HH imaging test score, using a logical OR of the eight previous measurements (P means DILI positive, N means DILI negative). This procedure assigned a DILI positive label to a compound if any single imaging measurement falls outside of the DILI negative threshold. All of these drugs were tested at 100-fold human therapeutic Cmax. The Cmax values for these drugs are listed in the rightmost column.

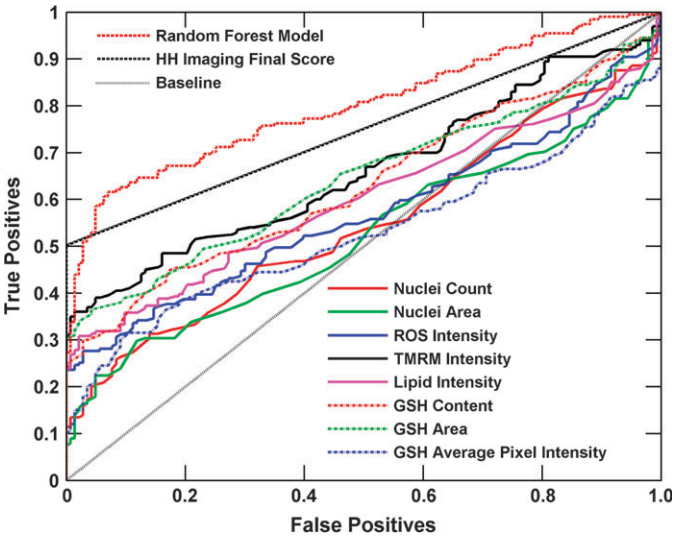

FIG. 2. ROC curve of individual and combined assay predictivity. The curve traces both true-positive and false-positive rates for all possible thresholds for each imaging assay measurement (Lasko *et al*., 2005). The top black and red dashed curves show the best combined results. They represent the ''HH Imaging Final Score'' and ''Random Forest Model,'' respectively (see main text for details). The bottom dotted curve shows the results of random assignment of toxicity (i.e., a ''coin toss'' baseline prediction of toxicity). Drug classification: positive = DILI positive = hepatotoxic.

uncertainty factor was used to account for higher drug exposure to the liver via liver portal vein for an orally dosed drug (Ito *et al*., 2002). We used a final threefold uncertainty factor to account for drug-drug or drug-diet interactions due to increased usage of polypharmacy (Routledge *et al*., 2004), naturaceuticals (Singh, 2005), and potential for increased drug exposure upon multiple days of dosing compared to the single-dose Cmax values used in this study. Therefore, whenever possible, orally dosed drugs were evaluated at a combined 100-fold of the Cmax values that were annotated in our DILI database. In a small fraction of cases where human therapeutic Cmax values were not reported, that drug or chemical was tested at 100μM (i.e., assuming a human single-dose therapeutic Cmax of 1μM). In a dose-response study, it was found that the 100-fold Cmax scaling factor represented a reasonable threshold to differentiate safe vs. toxic drugs (see Table 3 of the supplementary material on line). Such an expanded dose-response and/or time-response studies may be useful to identify signals of initiating injury, thus leading to further mechanistic exploration of hepatic damage.

The Importance of Mitochondria and Cellular Redox States to Organ Injury

Three features contributed most to the overall random forest model. They are, in decreasing order of importance: MMP, ROS, and reduced intracellular GSH level. These features, evaluated for the first time across so many drugs in a simultaneous and multiplexed fashion, reinforce the notion that alterations in mitochondrial energetics and cellular redox states are important mechanisms of drug-induced hepatotoxicity. These alterations may not be independent or mutually exclusive in the biological sense, as ROS generated at lower drug dose may be a prelude to mitochondrial damage and GSH depletion at a higher dose (e.g., see Supplementary Table 3). HIAT is designed to measure a panel of the most common mechanisms of toxicity, not the end result of cell death *per se*. While cytotoxicity may play a role in some of the more toxic compounds, the more subtle changes (e.g., ROS generation) can only be measured when cellular membranes are still intact.

It was postulated that mitochondrion plays a key role in idiosyncratic liver injury (reviewed by, Boelsterli and Lim, 2007; Kass and Price, 2008, and references therein). The mitochondrial hypothesis implies that initially silent but gradually accumulating mitochondrial injury in hepatocytes can reach a critical threshold and abruptly trigger liver injury. This hypothesis is consistent with the clinical findings that idiosyncratic DILI is typically delayed (by weeks or months), that among others both increasing age and polymorphisms in the mitochondrial form of the manganese superoxide dismutase are risk factors (Boelsterli and Lim, 2007), and that many DILI positive drugs in our database clearly exhibit a mitochondrial hazard *in vitro*. In parallel, oxidative stress is clearly involved in an animal model of delayed onset DILI, and anti-oxidant treatments such as resveratrol have consistently demonstrated *in vivo* protection in this model (Kasdallah-Grissa *et al*., 2007; Saravanan *et al*., 2007). Oxidative stress is also implicated in cholestatic liver disorders and hepatitis C infections (Choi and Ou, 2006; Sokol *et al*., 2006), and these pre-existing conditions are known to sensitize the liver to additional drug-induced damage. Our experimental findings are consistent with the hypothesis that many ''idiosyncratic'' drug reactions indeed cause subtle insults to the liver that are typically masked by a ''normal'' threshold of this highly adaptable organ. Only when such a ''normal'' threshold is genetically or epigenetically altered does frank liver toxicity emerge (Li, 2002; Uetrecht, 2008; Ulrich, 2007; Watkins, 2005).

A Low False-Positive Rate toward Serious Clinical DILI

The fact that the prediction of HIAT to serious clinical DILI as identified by Hy's Law has a very low false-positive rate made this testing strategy worthy of routine implementation in the drug discovery and development process. In particular, there are no shortages of clinically beneficial drugs that can cause a transient increase in serum alanine aminotransferase (ALT) activity without an increase in total serum bilirubin (TBL) concentration, and they do not cause serious hepatotoxicity in the clinic. Well-known examples of such drugs include tacrine, simvastatin, aspirin, fluoxetine, propranolol, raloxifene, paroxetine, and buspirone (FDA, 2007; Lee and Senior, 2005; Senior, 2007). These drugs should be classified as DILI negatives, as we did in this article. They were tested

and scored as negatives in the HIAT (Table 1). Hence the final conclusions from HIAT are distinct from what have been published about these drugs in the past (Chen *et al*., 2002; Galisteo *et al*., 2000; Kalgutkar *et al*., 2005; Laville *et al*., 2004; O'Brien *et al*., 2006; Pessayre *et al*., 1999; Tavintharan *et al*., 2007; Xu *et al*., 2003; Zhao *et al*., 2007). The reason for the high specificity of the HIAT may be a combination of (1) the drug concentrations used have reasonable relevance to the *in vivo* situation (e.g., 100x Cmax for an orally dosed drug), (2) primary hepatocytes are nondividing cells and compared to hepatoma cell lines are less sensitive to agents that may perturb the cell cycle (Holownia and Braszko, 2004); (3) primary hepatocyte culture in the sandwiched configuration maintains more normal and balanced drug-metabolizing and transporter functions (Bi *et al*., 2006; Gross-Steinmeyer *et al*., 2005; Hoffmaster *et al*., 2004; Page *et al*., 2007). The HIAT was evaluated against a large number of drugs (> 300 in total) with a significant number of DILI negative drugs, including those that cause a transient increase in ALT but not TBL (as discussed above). Therefore the exceptionally high specificity and positive predictive value reported here can probably be translated to a "real-world" scenario. The high positive predictive value toward the ultimate *in vivo* outcome (in this case serious DILI) is a striking contrast to the current *in vitro* tests for drug-induced genotoxicity (Kirkland *et al*., 2007), and should be a continued emphasis in developing, evaluating, and implementing *in vitro* test systems for the prediction of other drug-induced toxicity.

It should be noted that the current tests can detect "metabolic" (nonallergic) idiosyncratic toxicity, but not allergic idiosyncrasy that requires the presence of multiple cell types of the immune system. Further tests should be developed to detect allergic toxicity with a high degree of specificity. The 40–50% of drugs that were missed by the current test will become a fruitful area of future research. For example, clinical hepatotoxicity was observed with the combined usage of didanosine and stavudine, two nucleoside analogs that inhibit HIV reverse transcriptase. These two drugs by themselves were both negative in the current HIAT (see Supplementary Table 2). Future research should explore drug-drug combinations, longer-term treatment schedules, and additional imaging endpoints (e.g., mitochondrial DNA content, hepatobiliary transporter activity, etc.)

It is well-known that existing animal models are not very predictive of human DILI. The combined preclinical animal testing from rodents, dogs, and monkeys can only identify about half of hepatotoxic drugs in humans (Olson *et al*., 2000). By combining a well-defined model of primary human hepatocyte cultures and high content imaging technology, we have developed an *in vitro* testing approach that is capable of identifying many DILI positive drugs that were previously missed by animal testing. The cellular imaging technology described here is particularly powerful in identifying multiple mechanisms of drug-induced toxicity. It exhibits high specificity, and can be readily adapted and expanded upon by applying other cell types and/or other fluorescent or light-emitting indicators. Given the heightened attention to the issue of DILI by the FDA (2007) and EMEA (2008), the data presented here provide a new approach for future hepatotoxicity testing.

SUPPLEMENTARY DATA

Supplementary data are available online at http://toxsci.oxfordjournals.org/.

FUNDING

Pfizer Global Research and Development, Pfizer, Inc.

ACKNOWLEDGMENTS

We gratefully acknowledge the many helpful discussions and assistance by Pfizer colleagues in Systems Biology, Molecular Informatics and Research Informatics, and Drug Safety Research & Development, esp. Drs Jason Hughes, Robert Stanton, Sergio Rotstein, and Denise Robinson-Gravatt.

REFERENCES

Aithal, G. P., and Day, C. P. (2007). Nonsteroidal anti-inflammatory drug-induced hepatotoxicity. *Clin. Liver Dis.* **11,** 563–575.

Berson, A., De Beco, V., Letteron, P., Robin, M. A., Moreau, C., El Kahwaji, J., Verthier, N., Feldmann, G., Fromenty, B., and Pessayre, D. (1998). Steatohepatitis-inducing drugs cause mitochondrial dysfunction and lipid peroxidation in rat hepatocytes. *Gastroenterology* **114,** 764–774.

Bi, Y. A., Kazolias, D., and Duignan, D. B. (2006). Use of cryopreserved human hepatocytes in sandwich culture to measure hepatobiliary transport. *Drug Metab. Dispos.* **34,** 1658–1665.

Boelsterli, U. A. (2002). Mechanisms of NSAID-induced hepatotoxicity: Focus on nimesulide. *Drug Saf.* **25**(9), 633–648.

Boelsterli, U. A., and Lim, P. L. (2007). Mitochondrial abnormalities—A link to idiosyncratic drug hepatotoxicity? *Toxicol. Appl. Pharmacol.* **220,** 92–107.

Breiman, L. (2001). Random forests. *Machine Learn.* **45,** 5–32.

Chen, Q., Ngui, J. S., Doss, G. A., Wang, R. W., Cai, X., DiNinno, F. P., Blizzard, T. A., Hammond, M. L., Stearns, R. A., Evans, D. C., Baillie, T. A., and Tang, W. (2002). Cytochrome P450 3A4-mediated bioactivation of raloxifene: Irreversible enzyme inhibition and thiol adduct formation. *Chem. Res. Toxicol.* **15,** 907–914.

Choi, J., and Ou, J. H. (2006). Mechanisms of liver injury. III. Oxidative stress in the pathogenesis of hepatitis C virus. *Am. J. Physiol. Gastrointest. Liver Physiol.* **290,** G847–G851.

Choi, S. (2003). Nefazodone (Serzone) withdrawn because of hepatotoxicity. *CMAJ* **169,** 1187.

Davila, J. C., Xu, J. J., Hoffmaster, K. A., O'Brien, P. J., and Strom, S. C. (2007). Chapter 1. Current in vitro systems used to address drug-induced

liver injury. In *Hepatotoxicity: From Genomics to In vitro and In Vivo* (S. Sahu, Ed.). Wiley & Sons, New York.

Dorne, J. L., Walton, K., and Renwick, A. G. (2005). Human variability in xenobiotic metabolism and pathway-related uncertainty factors for chemical risk assessment: A review. *Food Chem. Toxicol.* **43,** 203–216.

Duda, P. O., Hart, P. E., Marroquin, L. D., Nadanaciva, S., Xu, J. J., Dunn, M. C., Smith, A. R., and Will, Y. (2000). In *Pattern Classification*. Wiley, New York.

Dykens, J. A., Jamieson, J. D., Marroquin, L. D., Nadanaciva, S., Xu, J. J., Dunn, M. C., Smith, A. R., and Will, Y. (2008). In vitro assessment of mitochondrial dysfunction and cytotoxicity of nefazodone, trazodone and buspirone. *Toxicol. Sci.* doi: 10.1093/toxsci/kfn56.

EMEA. (2008). Non-clinical guideline on drug-induced hepatotoxicity. Available at: http://www.emea.europa.eu/pdfs/human/swp/15011506en.pdf.

FDA. (2007). Drug-induced liver injury: Premarketing clinical evaluation. Available at: http://www.fda.gov/Cder/guidance/7507dft.htm.

Galisteo, M., Rissel, M., Sergent, O., Chevanne, M., Cillard, J., Guillouzo, A., and Lagadic-Gossmann, D. (2000). Hepatotoxicity of tacrine: Occurrence of membrane fluidity alterations without involvement of lipid peroxidation. *J. Pharmacol. Exp. Ther.* **294,** 160–167.

Giacomini, K. M., Krauss, R. M., Roden, D. M., Eichelbaum, M., Hayden, M. R., and Nakamura, Y. (2007). When good drugs go bad. *Nature* **446,** 975–977.

Gross-Steinmeyer, K., Stapleton, P. L., Tracy, J. H., Bammler, T. K., Lehman, T., Strom, S. C., and Eaton, D. L. (2005). Influence of Matrigel-overlay on constitutive and inducible expression of nine genes encoding drug-metabolizing enzymes in primary human hepatocytes. *Xenobiotica* **35,** 419–438.

Guggenheim, K. Y. (1993). Paracelsus and the science of nutrition in the renaissance. On occasion of the 500th anniversary of his birth. *J. Nutr.* **123,** 1189–1194.

Hewitt, N. J., Lechon, M. J., Houston, J. B., Hallifax, D., Brown, H. S., Maurel, P., Kenna, J. G., Gustavsson, L., Lohmann, C., Skonberg, C., *et al.* (2007). Primary hepatocytes: Current understanding of the regulation of metabolic enzymes and transporter proteins, and pharmaceutical practice for the use of hepatocytes in metabolism, enzyme induction, transporter, clearance, and hepatotoxicity studies. *Drug Metab. Rev.* **39,** 159–234.

Hoffmaster, K. A., Turncliff, R. Z., LeCluyse, E. L., Kim, R. B., Meier, P. J., and Brouwer, K. L. (2004). P-glycoprotein expression, localization, and function in sandwich-cultured primary rat and human hepatocytes: Relevance to the hepatobiliary disposition of a model opioid peptide. *Pharm. Res.* **21,** 1294–1302.

Holownia, A., and Braszko, J. J. (2004). Tamoxifen cytotoxicity in hepatoblastoma cells stably transfected with human CYP3A4. *Biochem. Pharmacol.* **67,** 1057–1064.

Holt, M. P., and Ju, C. (2006). Mechanisms of drug-induced liver injury. *AAPS J.* **8**(1), E48–E54.

Ito, K., Chiba, K., Horikawa, M., Ishigami, M., Mizuno, N., Aoki, J., Gotoh, Y., Iwatsubo, T., Kanamitsu, S., Kato, M., *et al.* (2002). Which concentration of the inhibitor should be used to predict in vivo drug interactions from in vitro data? *AAPS Pharm. Sci.* **4**(4), E25.

Kalgutkar, A. S., *et al.* (2005). Bioactivation of the nontricyclic antidepressant nefazodone to a reactive quinone-imine species in human liver microsomes and recombinant cytochrome P450 3A4. *Drug Metab. Dispos.* **33,** 243–253.

Kaplowitz, N. (2005). Idiosyncratic drug hepatotoxicity. *Nat. Rev. Drug Discov.* **4,** 489–499.

Kasdallah-Grissa, A., Mornagui, B., Aouani, E., Hammami, M., El May, M., Gharbi, N., Kamoun, A., and El-Fazaa, S. (2007). Resveratrol, a red wine polyphenol, attenuates ethanol-induced oxidative stress in rat liver. *Life Sci.* **80,** 1033–1039.

Kass, G. E. N., and Price, S. C. (2008). Role of mitochondria in drug-induced cholestatic injury. *Clin. Liver Dis.* **12,** 27–51.

Kirkland, D., Pfuhler, S., Tweats, D., Aardema, M., Corvi, R., Darroudi, F., Elhajouji, A., Glatt, H., Hastwell, P., Hayashi, M., *et al.* (2007). How to reduce false positive results when undertaking in vitro genotoxicity testing and thus avoid unnecessary follow-up animal tests: Report of an ECVAM Workshop. *Mutat. Res.* **628,** 31–55.

Kostrubsky, S. E., Strom, S. C., Kalgutkar, A. S., Kulkarni, S., Atherton, J., Mireles, R., Feng, B., Kubik, R., Hanson, J., Urda, E., *et al.* (2006). Inhibition of hepatobiliary transport as a predictive method for clinical hepatotoxicity of nefazodone. *Toxicol. Sci.* **90,** 451–459.

Lasko, T. A., Bhagwat, J. G., Zou, K. H., and Ohno-Machado, L. (2005). The use of receiver operating characteristic curves in biomedical informatics. *J. Biomed. Inform.* **38,** 404–415.

Laville, N., Ait-Aissa, S., Gomez, E., Casellas, C., and Porcher, J. M. (2004). Effects of human pharmaceuticals on cytotoxicity, EROD activity and ROS production in fish hepatocytes. *Toxicology* **196,** 41–55.

LeCluyse, E. L., Alexandre, E., Hamilton, G. A., Viollon-Abadie, C., Coon, D. J., Jolley, S., and Richert, L. (2005). Isolation and culture of primary human hepatocytes. *Methods Mol. Biol.* **290,** 207–229.

Lee, W. M. (2003). Drug-induced hepatotoxicity. *N. Engl. J. Med.* **349,** 474–485.

Lee, W. M., and Senior, J. R. (2005). Recognizing drug-induced liver injury: Current problems, possible solutions. *Toxicol. Pathol.* **33,** 155–164.

Li, A. P. (2002). A review of the common properties of drugs with idiosyncratic hepatotoxicity and the "multiple determinant hypothesis" for the manifestation of idiosyncratic drug toxicity. *Chem. Biol. Interact.* **142,** 7–23.

Navarro, V. J., and Senior, J. R. (2006). Drug-related hepatotoxicity. *N. Engl. J. Med.* **354,** 731–739.

O'Brien, P. J., Irwin, W., Diaz, D., Howard-Cofield, E., Krejsa, C. M., Slaughter, M. R., Gao, B., Kaludercic, N., Angeline, A., Bernardi, P., *et al.* (2006). High concordance of drug-induced human hepatotoxicity with in vitro cytotoxicity measured in a novel cell-based model using high content screening. *Arch. Toxicol.* **80,** 580–604.

Olson, H., Betton, G., Robinson, D., Thomas, K., Monro, A., Kolaja, G., Lilly, P., Sanders, J., Sipes, G., Bracken, W., *et al.* (2000). Concordance of the toxicity of pharmaceuticals in humans and in animals. *Regul. Toxicol. Pharmacol.* **32,** 56–67.

Page, J. L., Johnson, M. C., Olsavsky, K. M., Strom, S. C., Zarbl, H., and Omiecinski, C. J. (2007). Gene expression profiling of extracellular matrix as an effector of human hepatocyte phenotype in primary cell culture. *Toxicol. Sci.* **97,** 384–397.

Pessayre, D., Mansouri, A., Haouzi, D., and Fromenty, B. (1999). Hepatotoxicity due to mitochondrial dysfunction. *Cell Biol. Toxicol.* **15,** 367–373.

Powers, J. (2007). SBIR conference. Available at: http://grants.nih.gov/grants/funding/SBIRConf2007/SBIRConf2007_%20Powers.ppt [accessed May 28th, 2007] (No events in 3000 patients rules out risk of 1:1000 [compared to background hepatotoxicity risk of 1:1,000,000]).

Ross, D. B. (2007). The FDA and the case of Ketek. *N. Engl. J. Med.* **356**(16), 1601–1604.

Routledge, P. A., O'Mahony, M. S., and Woodhouse, K. W. (2004). Adverse drug reactions in elderly patients. *Br. J. Clin. Pharmacol.* **57,** 121–126.

Saravanan, N., Rajasankar, S., and Nalini, N. (2007). Antioxidant effect of 2-hydroxy-4-methoxy benzoic acid on ethanol-induced hepatotoxicity in rats. *J. Pharm. Pharmacol.* **59,** 445–453.

Scheen, A. J. (2001). Thiazolidinediones and liver toxicity. *Diabetes Metab.* **27,** 305–313.

Schuster, D., Laggner, C., and Langer, T. (2005). Why drugs fail—a study on side effects in new chemical entities. *Curr. Pharm. Des.* **11**(27), 3545–3559.

Senior, J. R. (2007). Drug hepatotoxicity from a regulatory perspective. *Clin. Liver Dis.* **11,** 507–524.

Shah, R. R. (2006). Can pharmacogenetics help rescue drugs withdrawn from the market? *Pharmacogenomics* **7,** 889–908.

Singh, Y. N. (2005). Potential for interaction of kava and St. John's wort with drugs. *J. Ethnopharmacol.* **100**(1–2), 108–113.

Sokol, R. J., Devereaux, M., Dahl, R., and Gumpricht, E. (2006). Let there be bile"—Understanding hepatic injury in cholestasis. *J. Pediatr. Gastroenterol. Nutr.* **43**(Suppl. 1), S4–S9.

Stricker, B. H. C. Ed. (1992). In *Drug-Induced Hepatic Injury*. Elsevier, Amsterdam.

Tavintharan, S., Ong, C. N., Jeyaseelan, K., Sivakumar, M., Lim, S. C., and Sum, C. F. (2007). Reduced mitochondrial coenzyme Q10 levels in HepG2 cells treated with high-dose simvastatin: A possible role in statin-induced hepatotoxicity? *Toxicol. Appl. Pharmacol.* **223,** 173–179.

Temple, R. (2006). Hy's law: Predicting serious hepatotoxicity. *Pharmacoepidemiol. Drug Saf.* **15,** 241–243.

Temple, R. J. (2001). Hepatotoxicity through the Years Impact on the FDA. Drug-induced liver toxicity. Silver Spring, MD Available at: http://www.fda.gov/cder/livertox/Presentations/im1389/sld003.htm. Accessed June 13, 2008.

Thiim, M., and Friedman, L. S. (2003). Hepatotoxicity of antibiotics and antifungals. *Clin. Liver Dis.* **7,** 381– 399; vi–vii.

Uetrecht, J. (2008). Idiosyncratic drug reactions: Past, present, and future. *Chem. Res. Toxicol.* **21,** 84–92.

Ulrich, R. G. (2007). Idiosyncratic toxicity: A convergence of risk factors. *Annu. Rev. Med.* **58,** 17–34.

Watkins, P. B. (2005). Idiosyncratic liver injury: Challenges and approaches. *Toxicol. Pathol.* **33,** 1–5.

Xu, J., Ma, M., and Purcell, W. M. (2003). Characterisation of some cytotoxic endpoints using rat liver and HepG2 spheroids as in vitro models and their application in hepatotoxicity studies. II. Spheroid cell spreading inhibition as a new cytotoxic marker. *Toxicol. Appl. Pharmacol.* **189,** 112–119.

Xu, J. J., Diaz, D., and O'Brien, P. J. (2004). Applications of cytotoxicity assays and pre-lethal mechanistic assays for assessment of human hepatotoxicity potential. *Chem. Biol. Interact.* **150,** 115–128.

Zhao, S. X., Dalvie, D. K., Kelly, J. M., Soglia, J. R., Frederick, K. S., Smith, E. B., Obach, R. S., and Kalgutkar, A. S. (2007). NADPH-dependent covalent binding of [3H]paroxetine to human liver microsomes and S-9 fractions: Identification of an electrophilic quinone metabolite of paroxetine. *Chem. Res. Toxicol.* **20,** 1649–1657.

Zimmerman, H. (1999). In *Hepatotoxicity: The Adverse Effects of Drugs and other Chemicals on the Liver*. Lippincott Williams & Wilkins, Philadelphia, PA.

Zimmerman, H. J. (2000). Drug-induced liver disease. *Clin. Liver Dis.* **4**(1), 73– 96, vi.